Poly(*N*-vinylcarbazole)–Clay Nanocomposite Materials Prepared by Photoinitiated Polymerization with Triarylsulfonium Salt Initiator

Yuan-Hsiang Yu[1,2], Ching-Yi Lin,[1] Jui-Ming Yeh[1]

[1]*Department of Chemistry and Center for Nanotechnology, Chung-Yuan Christian University, Chung Li, Taiwan 320, China*
[2]*Department of Electronic Engineering, Lan-Yan Institute of Technology, I-Lan 261, Taiwan, China*

Received 19 November 2002; accepted 1 July 2003

ABSTRACT: A series of polymer–clay nanocomposite (PCN) materials that consist of poly(*N*-vinylcarbazole) (PNVC) and layered montmorillonite (MMT) clay are prepared by effectively dispersing the inorganic nanolayers of MMT in an organic PNVC matrix via *in situ* photoinitiated polymerization with triarylsulfonium salt as the initiator. Organic NVC monomers are first intercalated into the interlayer regions of the organophilic clay hosts, followed by one-step UV-radiation polymerization. The as-synthesized PCN materials are typically characterized by Fourier transform IR spectroscopy, wide-angle X-ray diffraction, and transmission electron microscopy. The molecular weights of PNVCs extracted from the PCN materials and the bulk PNVC are determined by gel permeation chromatography analysis with tetrahydrofuran as the eluant. The morphological image of the synthesized materials is observed by an optical polarizing microscope. The effects of the material composition on the optical properties and thermal stability of PNVCs and a series of PCN materials (solution and fine powder) are also studied by UV–visible absorption spectra measurements, thermogravimetric analysis, and differential scanning calorimetry, respectively. © 2003 Wiley Periodicals, Inc. J Appl Polym Sci 91: 1904–1912, 2004

Key words: nanocomposite; clay; poly(*N*-vinylcarbazole); triarylsulfonium salt

INTRODUCTION

Polymer–clay nanocomposite (PCN) materials have evoked intensive research interests lately because their unique physical properties are drastically different from their bulk counterparts and therefore create potential commercial applications. The historical development of the PCN materials can be traced back to the research work of the Toyota group in which nylon-6/clay nanocomposites showed enhanced modulus and strength without sacrificing other compensating properties such as the impact resistance.[1] Subsequently, several polymer–clay hybrid nanocomposite material systems were developed by the dispersion of alkylammonium-exchanged forms of montmorillonites (MMTs) in various polymeric matrices such as nylon,[1] poly(methyl methacrylate) (PMMA),[2] epoxy resin,[3] polyimide,[4] polystyrene,[5] and so forth. PCN materials are reported to boost the thermal,[6] mechanical,[7] molecular barrier,[8] flame retardant,[9] and corrosion protection properties[10–12] of polymers at low clay loading.

Correspondence to: Prof. J.-M. Yeh (raymond3@tpts5.seed.net.tw).

Contract grant sponsor: NSC; Contract grant number: 89-2113-M-033-014.

Journal of Applied Polymer Science, Vol. 91, 1904–1912 (2004)

Conjugated polymers attracted considerable attention because they exhibit distinguish photoelectronic properties upon doping. In the doping process the conductivity of conjugated polymers can be changed from insulating to semiconducting to metallic regimes. The well-studied conducting conjugated polymers are usually classified into three major families: polyaromatic hydrocarbons, polyenes, and polyheterocycles. Polycarbazole (a heterocyclic polymer) has drawn much attention in the past decade.[13,14] Moreover, carbazole-containing polymers have been the subject of many studies because of their electro- and photochemical properties, as well as the high thermal stability of the carbazole system.[15,16] Recently, PCN materials that consist of poly(*N*-vinyl carbazole) (PNVC) and layered materials were found to display a novel property, which can be observed from two dissimilar chemical components combining at the molecular level.[17] However, *in situ* photoinitiated polymerization of PNVC–clay nanocomposite (PCN) materials and their related properties have not been reported.

In this study we prepare a series of PCN materials by effectively dispersing the inorganic nanolayers of MMT clay in the organic PNVC matrix via photoinitiated polymerization with triarylsulfonium hexafluoroantimonate as the initiator. The as-synthesized PCN materials are characterized by Fourier transform IR (FTIR) spectroscopy, wide-angle X-ray diffraction (WAXD), and transmission electron microscopy

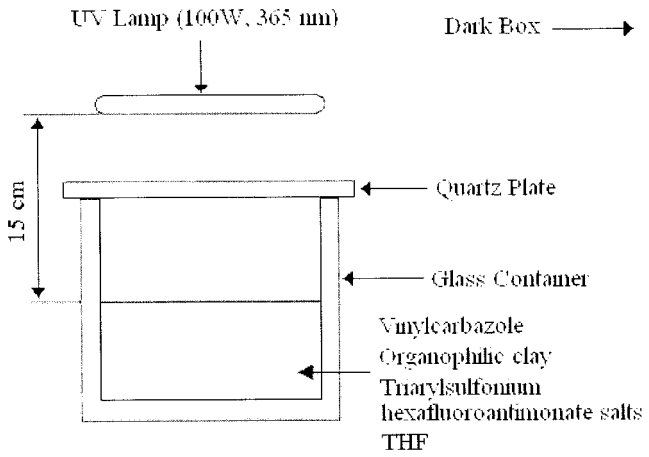

Figure 1 The Photochemical polymerization apparatus.

(TEM). The molecular weights of the PNVC extracted from the PCN materials and bulk PNVC are determined by gel permeation chromatography (GPC) analyses with THF as the eluant. The morphological images of the synthesized materials are studied with a polarizing microscope. The effects of the material composition on the thermal stability and optical properties of PNVC and a series of PCN materials in fine powder and solution forms are also studied by thermogravimetric analysis (TGA), differential scanning calorimetry (DSC), and UV–visible absorption spectra, respectively.

EXPERIMENTAL

Materials and methods

Diallylamine (98%, Lancaster), methanol (ACS grade, Tedia), NVC (98%, Aldrich), triarylsulfonium hexafluoroantimonate salt (Aldrich), PMMA (weight-average molecular weight = 350,000, Acros), lithium chloride (99%, Acros), and tetrahydrofuran (THF, 99%, Merck) were used as received without further purification. Hydrochloric acid (37%, Riedel–de Haën) was applied to prepare the 1.0*M* HCl aqueous solution. The MMT clay consisted of a cationic-exchange capacity (CEC) value of 98 meq/100 g and the unit cell formula $[Na_{0.48}K_{0.01}Ca_{0.01}Ti_{0.01}](Fe_{0.20}Al_{1.44}Mg_{0.31})(Si_{3.39}Al_{0.07})O_{10}(OH)_2 \cdot 2H_2O$ as provided by Pai-Kong Ceramic Company (Taiwan).

The apparatus for photochemical polymerization is shown in Figure 1. A UV lamp (CA91786, P/N 95-0127-01, Upland) in a dark box was used for the experiment (365-nm wavelength, 100-W power). The FTIR spectra were recorded from pressed KBr pellets using a Bio-Rad FTS-7 FTIR spectrometer. The powder WAXD study of the samples was carried out with a Rigaku D/MAX-3C OD-2988N X-ray diffractometer with a copper target and Ni filter at a scanning rate of 4°/min. The samples for the TEM study were first prepared by putting PCN powder into PMMA capsules and curing the PMMA at 100°C for 24 h in a vacuum oven. Then the cured PMMA-containing PCN materials were microtomed with a Reichert–Jung Ultracut-E into 60–90 nm thick slices. Subsequently, one layer of carbon (~10 nm thick) was deposited on these slices on 100 mesh copper nets for TEM observations on a JEOL-200FX with an acceleration voltage of 120 kV. The morphological images of the as-synthesized materials were evaluated by an Olympus DP10 polarizing microscope. The molecular weight of the polymer extracted from all samples and the bulk PNVC was determined by GPC. A Waters GPC model 2 II equipped with a programmable solvent delivery module (model 590), a differential refractometer detector, and a Styragel HT column were employed to perform the GPC studies. The UV–visible transmission spectra of the polymer in solution form were recorded on a Hitachi U-2000 UV–visible spectrometer at room temperature. A Seiko thermal analysis system equipped with a TGA/SDTA 851 and a DSC-910S was employed to perform the thermal analyses under N_2 flow at a flow rate of 20 mL/min. The programmed heating rate was 10°C/min.

Preparation of organophilic clay

Organophilic clay is prepared[10–12] by a cationic-exchange reaction between the sodium cations of the MMT clay and the alkylammonium ions of the intercalating agent, diallylamine. Typically, 5 g of MMT clay with a CEC value of 98 meq/100 g is stirred in 800 mL of distilled water (beaker A) at room temperature for 24 h. A separate solution containing 0.571 g of intercalating agent in another 100 mL of distilled water (beaker B) is magnetically stirred, followed by adding a 1.0*M* HCl aqueous solution to adjust the pH value to about 3–4. After stirring for 1 h, the protonated amino acid solution (beaker B) is added to the MMT suspension (beaker A) at a rate of approximately 10 mL/min with vigorous stirring. The mixture is stirred for 24 h at room temperature. The organophilic clay is recovered by ultracentrifuging (9000 rpm for 30 min) and filtering the solution in a Buchner funnel. The purification of the products is performed by washing and filtering the samples at least 3 times to remove any excess ammonium ions. Upon drying under a dynamic vacuum for 48 h, the organophilic clay is obtained.

Photochemical preparation of PNVC and PCN materials

As a typical procedure for the preparation of PNVC or PCN materials via photochemical polymerization, an appropriate amount of organophilic clay, which is calculated as 0 wt % (0 g, for PNVC), 0.25 wt % (0.025

TABLE I
Relations of Composition of PNVC-MMT Clay Nanocomposite Materials to Molecular Weights, UV–Visible Absorbance Wavelength, and Thermal Stability by GPC, UV–visible, TGA, and DSC Measurements

Compound code	Feed composition (wt%)		Molecular weights[a]			UV–visible data[b]		Thermal analyses	
	N-Vinyl carbazole	Clay	M_w	M_n	PD	Band I (nm)	Band II (nm)	T_d (°C)[c]	T_g (°C)[d]
PNVC	100	0	2768	2273	1.22	256	330	215.36	48.25
CLNVC0.25	99.75	0.25	2028	1761	1.15	254	325	173.45	56.37
CLNVC0.5	99.5	0.5	1725	1542	1.12	253	323	175.77	69.18
CLNVC0.75	99.25	0.75	1658	1503	1.10	250	320	180.90	75.46
CLNVC1	99	1	1569	1438	1.09	248	319	191.34	78.45

[a] As determined by GPC with THF as the eluant.
[b] As determined by UV–visible absorbance spectra measurements.
[c] As determined by TGA.
[d] As determined by DSC.

g), 0.5 wt % (0.05 g), 0.75 wt % (0.075 g), and 1 wt % (0.1 g) with respect to NVC, is introduced into 100 mL of THF under magnetic stirring for 24 h at room temperature. The NVC monomers, which are calculated as 100 wt % (10 g, for PNVC), 99.75 wt % (9.975 g), 99.5 wt % (9.95 g), 99.25 wt % (9.925 g), and 99 wt % (9.9 g), respectively, are subsequently added to the dispersed organophilic clay solution. The mixture is then stirred for 24 h at room temperature. Upon the addition of the initiator triarylsulfonium hexafluoroantimonate salt (1/1000 mol ratio with respect to NVC monomer), the solution is transferred to a glass container for photochemical polymerization. After radiation by a UV lamp (365-nm wavelength and 100-W power) housed in a light-proof box for 24 h at room temperature, the PNVC or PCN precipitates are obtained.

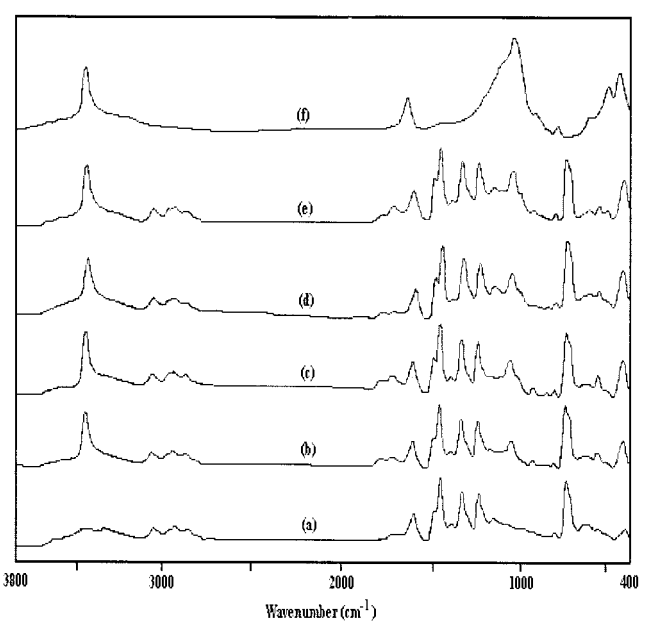

Figure 2 Representative FTIR spectra of PNVC (spectrum a), CLNVC0.25 (spectrum b), CLNVC0.5 (spectrum c), CLNVC0.75 (spectrum d), CLNVC1 (spectrum e), and organophilic clay (spectrum f).

Polymer recovery

A reverse cationic-exchange reaction is employed to separate bound PNVC from the inorganic component in the nanocomposite.[18] As a typical extraction procedure, 2 g of fine powder of synthesized PCN materials are dissolved in ~100 mL of THF (beaker A). A separate 10-mL stock solution of 1 wt % $LiCl_{(s)}$ in THF is prepared (beaker B). Both beakers are subjected to vigorous magnetic stirring for 3–4 h at room temperature. After combining the contents of the two beakers, the mixture is stirred for an additional 24 h followed by Soxhlet extraction at 85–90°C for 48 h. The extract solution is evaporated on a rotavapor under reduced pressure to yield PNVC fine powders. The molecular weights of both the extracted and bulk PNVC are determined by GPC analyses with THF as the eluant.

RESULTS AND DISCUSSION

NVC is a well-studied monomer that can be photopolymerized and therefore lead to a polymer (PNVC) with unusual electrical and photoelectronic properties and high thermal stability. During the past decade, numerous attempts have been made to chemically modify PVNC to produce potential materials with improved bulk properties.[19] In this study we prepared a series of PCN materials by photoinitiated polymerization and we evaluated their properties. The polymerization of NVC can proceed simultaneously by a combination of both cationic and free-radical mechanisms. The typical photochemical process with triphenylsulfonium hexafluoroantimonate as the initiator for the preparation of PNVC can be represented through the following reactions[20,21]:

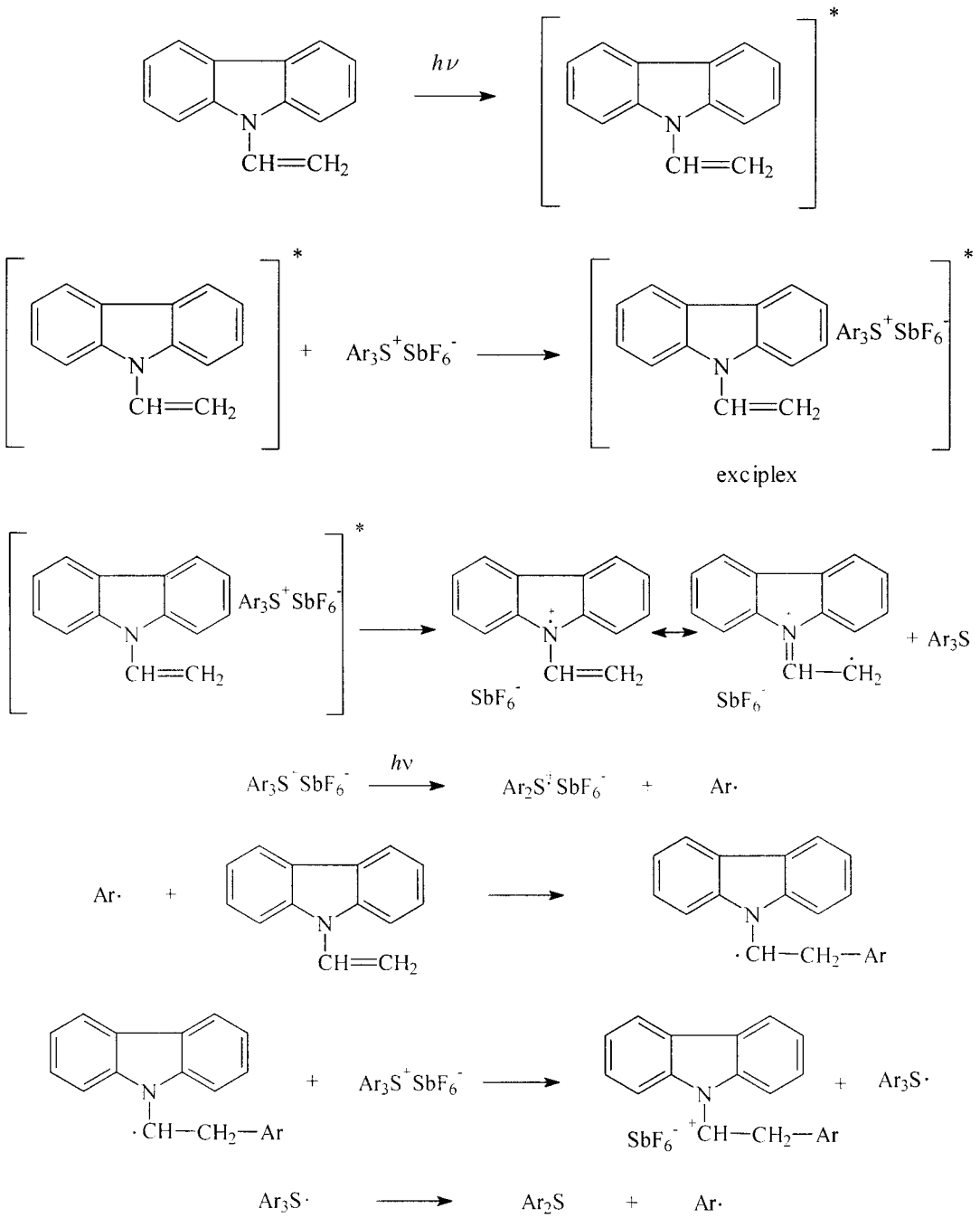

In contrast, MMT is a clay mineral containing stacked silicate sheets measuring ~10 Å in thickness and ~2180 Å in length.[22] It possesses a high aspect ratio and a platey morphology. The chemical structures of MMT consist of two fused silica tetrahedral sheets sandwiching an edge-shared octahedral sheet of either magnesium or aluminum hydroxide. The Na^+ and Ca^{+2} residing in the interlayer regions can be replaced by organic cations such as alkylammonium ions by a cationic-exchange reaction to modify the hydrophilic layer silicate into an organophilic one. MMT has a high swelling capacity, which is important for efficient intercalation of the polymer, and is composed of stacked silicate sheets that provide improved thermal stability, mechanical strength, fire retardant, and molecular barrier properties.

To synthesize the PCN materials, organophilic clay is first prepared by a cationic-exchange reaction between the sodium cations of MMT clay and the alkylammonium ions of the intercalating agent (diallylamine). Organic NVC monomers are subsequently intercalated into the interlayer regions of organophilic clay hosts, which is followed by one-step photochemical polymerization with an initiator (triarylsulfonium hexafluoroantimonate salt). The apparatus for photo-

chemical polymerization is illustrated as Figure 1. The composition of the PCN materials is varied from 0 to 1 wt % clay with respect to the PNVC content as summarized in Table I.

Characterization

The representative FTIR spectra of the organophilic clay, neat PNVC, and PCN materials are given in Figure 2. The characteristic vibration bands of PNVC[23] are shown at 1605 and 1480 (aromatic ring —C═C— stretch), 1230 (C—H in-plane deformation of the aromatic ring), and 753 cm^{-1} (ring deformation of the aromatic structure). Those of diallylamine–MMT clay[10–12] are shown at 3489 (—NH), 1650 (C═C), 802 ($—CH_2$), 1043 (Si—O), 518 (Al—O), and 468 cm^{-1} (Mg—O). As the loading of organophilic MMT clay is increased, the intensities of the organophilic MMT clay bands become stronger in the FTIR spectra of PCN materials.

Figure 3 illustrates the powder WAXD patterns of organophilic clay and a series of PCN materials. In Figure 3(A) the powder WAXD patterns from 2θ = 2–10° do not show any diffraction peak below the diffraction peak at 2θ = 6.35° (d-spacing = 1.391 nm) for organophilic clay and 2θ = 7.45° (d-spacing = 1.185 nm) for MMT clay, indicating the possibility of having exfoliated silicate layers of organophilic clay dispersed in the PNVC matrix. However, there is a small diffraction peak appearing at 2θ = 9.1°, corresponding to a d-spacing of 0.97 nm for PNVC. The intensity of this peak is increased when the amount of organophilic clay increases for PCN materials. Furthermore, when the powder WAXD patterns are scanned from 2θ = 10 to 20° no diffraction peak appears for PNVC, whereas there are three intense diffraction peaks appearing at 2θ = 17.5°, 21.7°, and 26.3°. The intensity of these three peaks is also increased when the amount of organophilic clay increases for PCN materials, as shown in Figure 3(B). This implies that the crystalline behavior of PNVC would be enhanced by loading of organophilic clay in the form of an intercalated or exfoliated layer structure. This is further evidenced by the studies of the morphological image of the synthesized materials with a polarizing microscope.

In Figure 4 the TEM of PCN materials with 1 wt % clay loading shows that the lamellar nanocomposite has a mixed nanomorphology. Individual silicate layers, along with two, three, and four layer stacks, are found to be exfoliating in the PNVC matrix. In addition, some larger intercalated tactoids can be identified.

Morphological image studies

The morphological image of the materials was studied with a polarizing microscope. For these studies the bulk PNVC and CLNVC1 (1 wt% clay loading in composite) fine powder are dissolved in THF to give typical 0.1 wt % solutions. After filtering, the as-prepared solutions are cast onto a microscope slide glass (1.0 × 1.0 cm) followed by drying in air for 24 h at 100°C to give coatings for conoscopy observation with the polarizing microscope. The polarizing microscope images in Figure 5 show a crystallite morphology for CLNVC1 that is different than the flat morphology of PNVC. The granule shape of CLNVC1 implies that some crystalline behavior occurred as the polymer

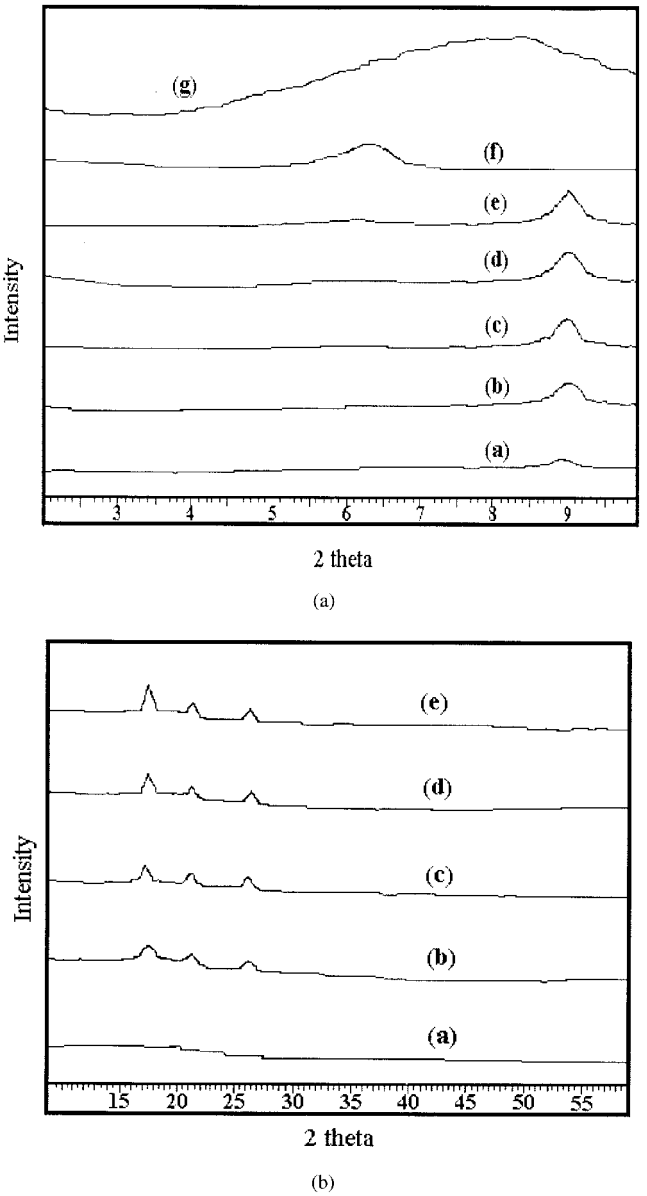

Figure 3 Wide-angle powder X-ray diffraction patterns of PNVC (spectrum a), CLNVC0.25 (spectrum b), CLNVC0.5 (spectrum c), CLNVC0.75 (spectrum d), CLNVC1 (spectrum e), organophilic clay (spectrum f), and clay (spectrum g) scanned from 2θ = (A) 2°–10° and (B) 10°–60°.

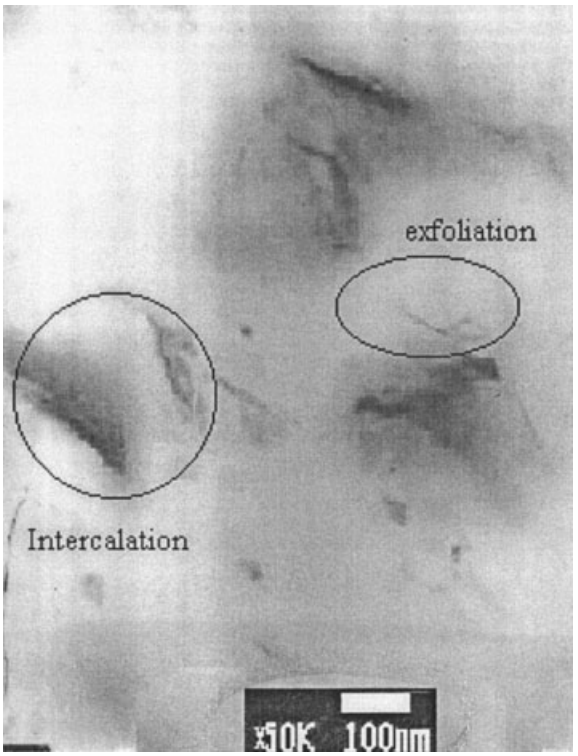

Figure 4 Transmission electron microscopy of CLNVC1.

incorporated MMT clay. This result is consistent with the powder WAXD patterns described previously.

Weight-average molecular weight of extracted and bulk PNVC

The molecular weights of the various polymer samples extracted from the nanolayers of MMT clays are obtained by GPC analyses. The molecular weights of the THF soluble polymer extracted from all samples, as well as the bulk PNVC, display monomodal peak distributions corresponding to a molecular weight value, as shown in Table I. The molecular weights of PCN materials decrease with increasing clay loading, indicating the structurally restricted polymerization conditions in the intragallery region of the MMT clay, as shown in Figure 6.[24] The proposed pathways for polymer chain propagation of pure PNVC and PCN materials are shown in Figure 7. Another possible explanation of the reduced polymer molecular weight with increasing clay content could be that the clay blocked the UV radiation during the photochemical polymerization process.

Optical properties of solution

Figure 8 shows the UV–visible absorbance spectra of pure PNVC and PCN materials in THF solutions. There are two absorbance bands observed at around 250 and 330 nm that may be attributed to π–π^* absorptions of the aromatic chromophores of the carbazole units in the polymer.[25] The wavelengths of pure PNVC and PCN materials in the UV–visible regions are gradually affected by the presence of clay loading

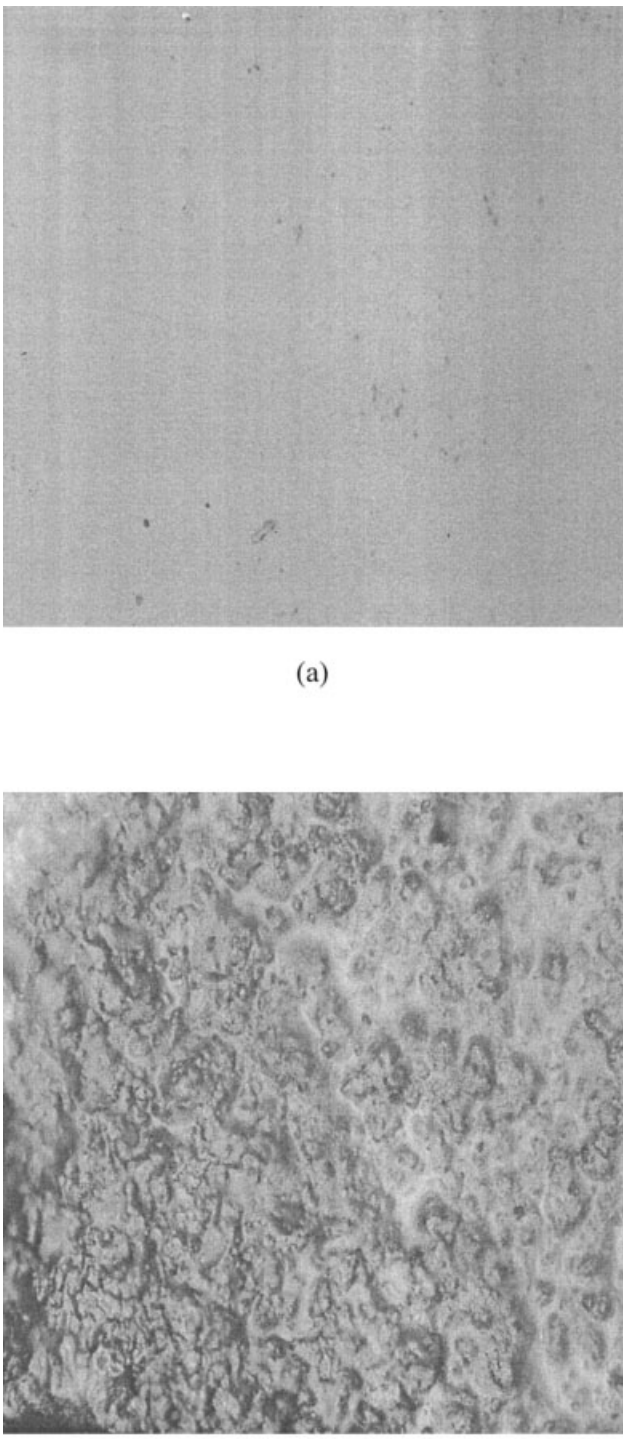

Figure 5 Polarizing microscope images of (a) PNVC and (b) CLNVC1.

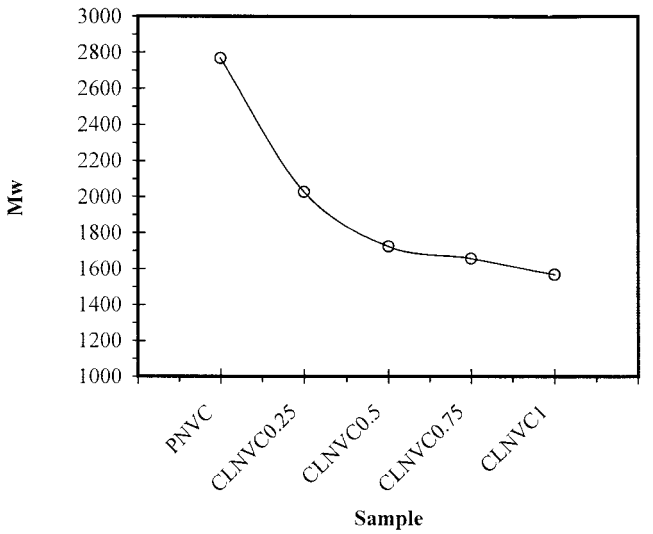

Figure 6 The relationships between the molecular weight and clay loading as obtained from GPC measurements.

in the PCN materials as illustrated in Table I. The spectra exhibiting blueshifts reflect the energy gap of the π–π^* transition increasing along with the MMT loading.[26] This may be attributed to the molecular weight decrease of PCN materials, which is consistent with that mentioned above.

Thermal properties of fine powders

Figure 9 shows a typical TGA thermogram of the weight loss as a function of temperature for PCN materials and PNVC as measured under a nitrogen atmosphere. In general, major weight losses are observed in the range of ~150–550°C for PNVC and PCN fine powers, which may correspond to the structural decomposition of the polymers. Evidently, the thermal decomposition of those PCN materials shifts toward a lower temperature range than that of PNVC, as illustrated in Table I, which may be due to the molecular weight decrease of PCN materials. Furthermore, all the PCN materials show a further increased decomposition temperature along with the loading of MMT clay, which may confirm the enhancement of the thermal stability when the MMT clay content is increased.[27] After ~600°C, the curves all became flat and mainly the inorganic residues (i.e., Al_2O_3, MgO, SiO_2) remained.

DSC traces of PNVC and PCN materials are shown in Figure 10. PNVC exhibits an endotherm at 48.25°C, corresponding to the glass-transition temperature (T_g) of PNVC. All the PCN materials show a higher T_g, as shown in Table I, compared to pure PNVC. This is tentatively associated with the confinement of the intercalated polymer chains within the clay galleries that prevents the segmental motions of the polymer chains.

CONCLUSIONS

A series of nanocomposite materials that consisted of PNVC and layered MMT clay are prepared by effectively dispersing the inorganic nanolayers of the MMT clay in the organic PNVC matrix via photochemical polymerization of NVC monomers with triarylsulfonium hexafluoroantimonate salt (initiator). The synthesized PCN materials are characterized by FTIR, WAXD, and TEM. The morphological images of the PCN materials are studied with a polarizing microscope. Crystalline surface morphology is observed with the incorporation of MMT clay into the PNVC matrix. This is consistent with the observation of pow-

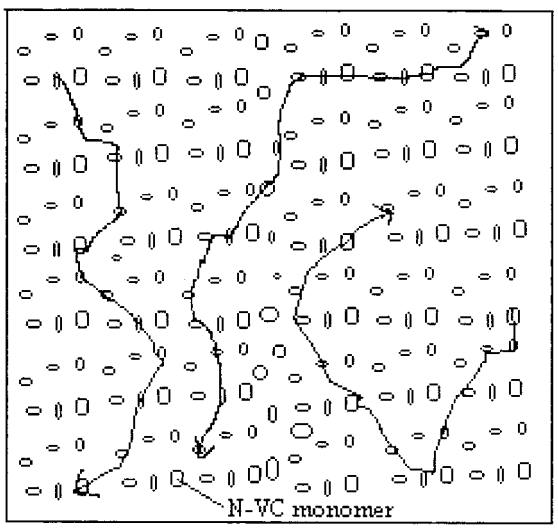

(a)

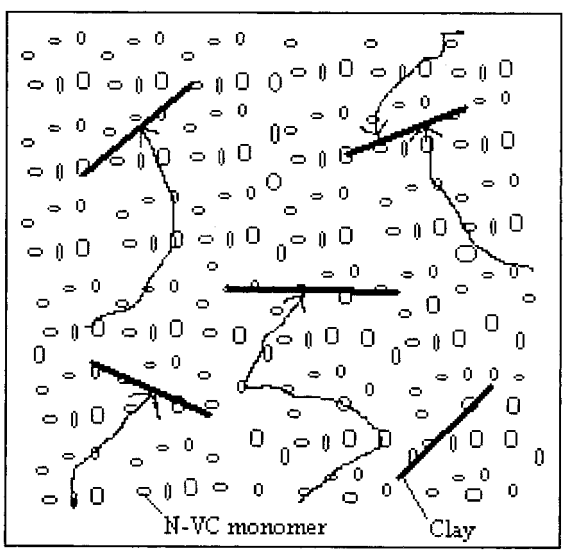

(b)

Figure 7 The proposed pathway for polymer chain propagation of (a) pure PNVC and (b) PNVC–clay nanocomposite materials.

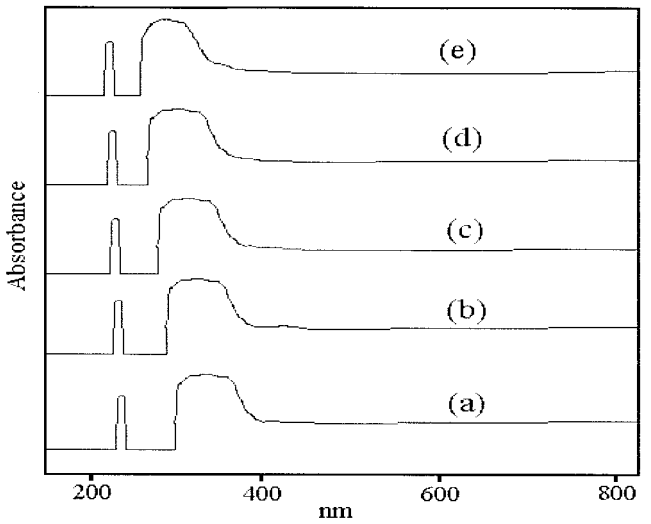

Figure 8 UV–visible spectra of PNVC (spectrum a), CLNVC0.25 (spectrum b), CLNVC0.5 (spectrum c), CLNVC0.75 (spectrum d), and CLNVC1 (spectrum e).

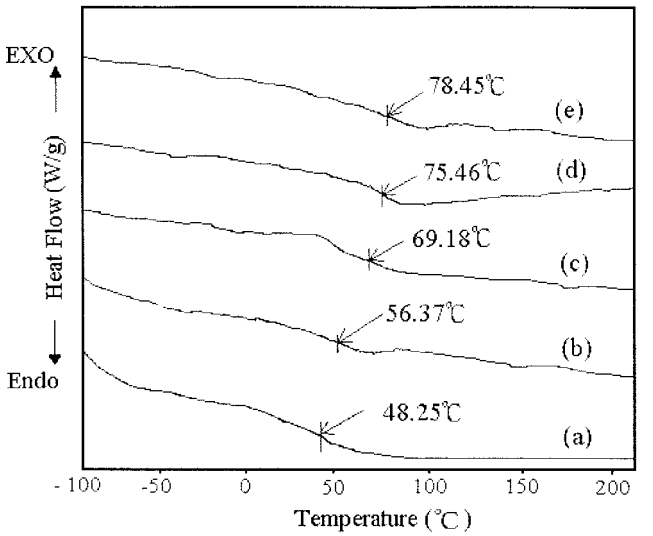

Figure 10 DSC curves of PNVC (curve a), CLNVC0.25 (curve b), CLNVC0.5 (curve c), CLNVC0.75 (curve d), CLNVC1 (curve e).

der WAXD patterns in which several intense peaks appearing for PCN materials are increased along with the loading of MMT clay.

The molecular weights of PNVC extracted from lamellar PCN materials and bulk PNVC are determined by GPC. The molecular weights of extracted PNVC exhibit a decreased molecular weight compared to the bulk PNVC, indicating the structurally restricted polymerization conditions in the intragallery region of the MMT clay. The optical properties and thermal stability of PNVC and a series of PCN materials (solution and fine powder forms) are also investigated by UV–visible absorption spectra, TGA, and DSC, respectively. The UV–visible absorption spectra exhibit a blueshift of the aromatic chromophores when the MMT content is increased. The thermal decomposition temperature of the PCN materials is lower than the bulk PNVC because of the decrease of the molecular weights with the incorporation of MMT clay. Increasing the nanolayers of MMT clay in the PCN matrix results in an increment in the thermal decomposition and glass-transition temperatures based on TGA and DSC studies.

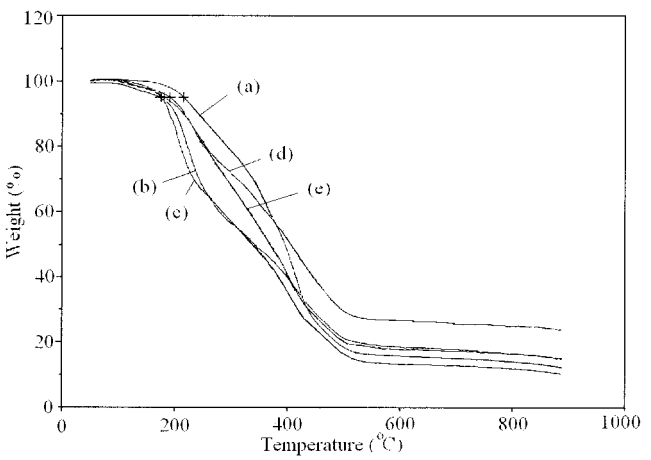

Figure 9 TGA curves of PNVC (curve a), CLNVC0.25 (curve b), CLNVC0.5 (curve c), CLNVC0.75 (curve d), and CLNVC1 (curve e).

The financial support of this research by the NSC is gratefully acknowledged.

References

1. Usuki, A.; Kawasumi, M.; Kojima, Y.; Okada, A.; Karauchi, T.; Kamigaito, O. J Mater Res 1993, 8, 1774.
2. Lee, D. C.; Jang, L. W. J Appl Polym Sci 1996, 61, 1117.
3. Lee, D. C.; Jang, L. W. J Appl Polym Sci 1998, 68, 1997.
4. Tyan, H.-L.; Liu, Y.-C.; Wei, K.-H. Chem Mater 1999, 11, 1942.
5. Akelah, A.; Rehab, A.; Selim, A.; Agag, T. J Mol Catal 1994, 94, 311.
6. Lan, T.; Kaviratna, P. D.; Pinnavaia, T. J. Chem Mater 1994, 6, 573.
7. Tyan, H.-L.; Liu, Y.-C.; Wei, K.-H. Chem Mater 1999, 11, 1942.
8. Wang, Z.; Pinnavaia, T. J. Chem Mater 1998, 10, 3769.
9. Gilman, J. W.; Jackson, C. L.; Morgan, A. B.; Hayyis, R., Jr.; Manias, E.; Giannelis, E. P.; Wuthenow, M.; Hilton, D.; Philips, S. H. Chem Mater 2000, 12, 1866.
10. Yeh, J.-M.; Liou, S.-J.; Lai, C.-Y.; Wu, P.-C.; Tsai, T.-Y. Chem Mater 2001, 13, 1131.
11. Yeh, J.-M.; Chen, C.-L.; Chen, Y.-C.; Ma, C.-Y.; Lee, K.-R.; Wei, Y.; Li, S. Polymer 2002, 43, 2729.
12. Yeh, J,-M.; Liou, S.-J.; Lin, C.-Y.; Cheng, C.-Y.; Chang, Y.-W.; Lee, K.-R. Chem Mater 2002, 14, 154.
13. Abthagir, P. S.; Dhanalak, S.-K.; Saraswathi, R. Synth Met 1998, 93, 1.

14. Verghese, M. M.; Ram, M. K.; Vardhan, H.; Malhotra, B. D.; Ashraf, S. M. Polymer 1997, 38, 1625.
15. Pennwell, R. C.; Ganguly, B. N.; Smith, T. W. J Polym Sci Macromol Rev 1973, 13, 63 and references therein.
16. Biswas, M.; Das, S. K. Polymer 1982, 23, 1705.
17. Mukul, B.; Suprakas, S. R. Polymer 1998, 39, 6423.
18. Meier, L. P.; Sheldon, R. A.; Caseri, W. R.; Suter, U. W. Macromolecules 1994, 27, 1637.
19. Biswas, M.; Mitra, P. J Appl Polym Sci 1991, 42, 1989.
20. Hua, Y.; Crivello, J. V. J Polym Sci Part A: Polym Chem 2000, 38, 3697.
21. Hua, Y.; Crivello, J. V. Macromolecules 2001, 34, 2488.
22. Yano, K.; Usuki, A.; Okada, A. J Polym Sci Part A: Polym Chem 1997, 35, 2289.
23. Sezer, E.; Ustamehmetoğlu, B.; Saraç, A. S. Synth Met 1999, 107, 7.
24. Wrobleski, D. A.; Benicewicz, B. C.; Thompson, K. G.; Byran, C. J. Polym Prepr 1994, 35, 265.
25. Chen, Y.; Yamamura, T.; Igarashi, K. J Polym Sci Part A: Polym Chem 2000, 38, 90.
26. Silverstein, R. M. Spectrometic Identification of Organic Compounds, 6th ed.; Silverstein, R. H.; Webster F. X., Eds. John Wiley & Sons: New York, 1998; p 291.
27. Lee, D. C.; Jang, L. W. J Appl Polym Sci 1996, 61, 1117.